

All-Optical Switch and Transistor Gated by One Stored Photon

Wenlan Chen,¹ Kristin M. Beck,¹ Robert Bücker,^{1,2} Michael Gullans,³ Mikhail D. Lukin,³ Haruka Tanji-Suzuki,^{1,3,4} Vladan Vuletić^{1*}

The realization of an all-optical transistor, in which one “gate” photon controls a “source” light beam, is a long-standing goal in optics. By stopping a light pulse in an atomic ensemble contained inside an optical resonator, we realized a device in which one stored gate photon controls the resonator transmission of subsequently applied source photons. A weak gate pulse induces bimodal transmission distribution, corresponding to zero and one gate photons. One stored gate photon produces fivefold source attenuation and can be retrieved from the atomic ensemble after switching more than one source photon. Without retrieval, one stored gate photon can switch several hundred source photons. With improved storage and retrieval efficiency, our work may enable various new applications, including photonic quantum gates and deterministic multiphoton entanglement.

Photons are excellent carriers of quantum information, but it is difficult to induce the strong interactions between individual photons that are required for, for example, all-optical quantum information processing. Nevertheless, advances toward such interactions have been made in cavity quantum electrodynamics (QED) systems with atoms (1–6) or artificial atoms (7–11) and in a cavity-free system by using atomic Rydberg states (12, 13) or dye molecules (14). All-optical switching of one beam by another (15) and cross-phase modulation (16) have been demonstrated at the level of a few hundred photons by means of electromagnetically induced transparency (EIT) (17–21). At the few-photon level, nonclassical light has been generated (1, 4, 6–9, 11–13, 22), and optical nonlinearities of 16° in phase shift (23) and up to ~20% in two-photon attenuation (5, 9, 10) have been observed in cavity QED systems. Although switching of the cavity transmission by a single atom has also been achieved (24), the realization of an optical transistor exhibiting gain with gate signals at the few- or one-photon level (25) remains a challenge.

We demonstrate a cavity QED version (18) of an optical switch (25) based on EIT in a four-level system (17–19) in which the collective atomic excitation associated with the storage of one gate photon (20, 26, 27) blocks the resonator transmission. Our system (5) consists of an ensemble of laser-cooled cesium atoms optically trapped inside a high-finesse optical cavity

(Fig. 1A) operating in the strong-coupling regime (1–6) of cavity QED. Each atom has a four-state N -type level structure $|g\rangle \leftrightarrow |d\rangle \leftrightarrow |s\rangle \leftrightarrow |e\rangle$ with two stable ground states, $|g\rangle$ and $|s\rangle$, and two electronic excited states, $|d\rangle$ and $|e\rangle$ (Fig. 1B). For atoms prepared in state $|g\rangle$, this atomic structure mediates an effective interaction between free-space photons (photons resonant with the $|g\rangle \rightarrow |d\rangle$ transition serving as gate photons) and cavity photons (photons resonant with the $|s\rangle \rightarrow |e\rangle$ transition serving as the source) (17–19). These two transitions are connected via a control laser that addresses the $|d\rangle \rightarrow |s\rangle$ transition and induces transparency (EIT) for the gate photons. By ramping the control laser power down to zero, we stored a weak gate pulse inside the atomic ensemble (Fig. 1B) and retrieved it at a later time by adiabatically reapplying the control beam (Fig. 1D) (20, 26, 27). In between storage and retrieval, we applied a source beam (Fig. 1C). The atomic population in state $|s\rangle$ associated with the stored gate pulse can block the transmission of the source pulse through the cavity (24). Because of the finite optical depth (OD) of the ensemble ($OD \leq 0.9$) and suboptimal control waveform (28), 1 out of 5 to 10 incident gate photons is stored.

We first characterized the cavity transmission without gate photon retrieval. To this end, we measured the average cavity transmission spectrum for different mean stored gate photon numbers $\langle n_g \rangle$ (Fig. 2). Because the gate pulses are weak classical pulses (coherent states), they are associated with Poissonian distributions in photon number n_g , and there is a finite probability $p(0) = e^{-\langle n_g \rangle}$ that the stored gate pulse does not contain any photons. Therefore, even if one photon were to perfectly switch off the source beam, there is a maximum average switching contrast $1 - e^{-\langle n_g \rangle}$ for measurements with coherent states of gate photons (Fig. 2, inset, solid line). The measured data points lie close to the maximum possible switch-

ing contrast and within the theoretically expected range (Fig. 2, gray area).

The photon number quantization of the gate pulse and the cavity blocking by just one gate photon are evident when we plot histograms of transmission spectra (Fig. 3) instead of the average transmission. The histogram shows two clearly separated components (Fig. 3B), where the high-transmission component corresponds to $n_g = 0$, whereas the low-transmission component corresponds to $n_g \geq 1$ (mostly $n_g = 1$ gate photons). The high-to-low peak transmission ratio gives an extinction factor for one stored gate photon of $T^{-1} = 11 \pm 1$.

In order to characterize the optical gain of the system, we measured the distribution of the

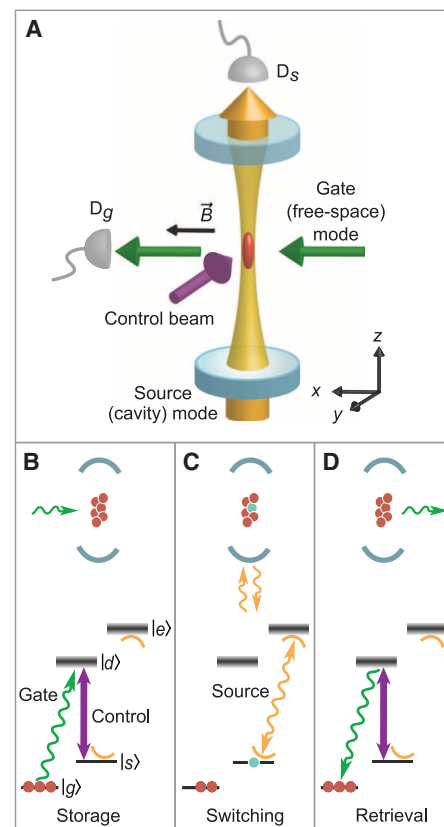


Fig. 1. All-optical switch and transistor. (A) Setup and **(B to D)** atomic level scheme with experimental sequence. An ensemble of laser-cooled atoms is trapped inside an optical resonator operating in the single-atom strong-coupling regime on the $|s\rangle \rightarrow |e\rangle$ transition. **(B)** We first stored a gate photon in the medium, which corresponds to a collective atomic excitation to state $|s\rangle$. **(C)** This collective excitation blocks the transmission of source photons through the cavity and **(D)** can be retrieved. Retrieved gate and transmitted source photons are measured with photon counters D_g and D_s , respectively. The atomic states of ^{133}Cs used in this experiment are $|g\rangle = |6S_{1/2}, F=3, m_F=3\rangle$, $|d\rangle = |6P_{3/2}, 4, 4\rangle$, $|s\rangle = |6S_{1/2}, 4, 4\rangle$, and $|e\rangle = |6P_{3/2}, 5, 5\rangle$, where F and m_F denote the hyperfine and magnetic sublevels, respectively.

¹Department of Physics and Research Laboratory of Electronics, Massachusetts Institute of Technology, Cambridge, MA 02139, USA. ²Vienna Center for Quantum Science and Technology, Atominstut, Technische Universität Wien, Stadionallee 2, 1020 Vienna, Austria. ³Department of Physics, Harvard University, Cambridge, MA 02138, USA. ⁴Photon Science Center, School of Engineering, University of Tokyo, 2-11-16 Yayoi, Bunkyo-ku, Tokyo 113-8656, Japan.

*Corresponding author. E-mail: vuletic@mit.edu

transmitted source photon number, $M_s = \frac{\mathcal{T}}{\mathcal{T} + \mathcal{L}} \int dt m_c(t) \kappa$, on cavity resonance. Here, $m_c(t)$ is the intracavity photon number at time t , κ is the cavity linewidth, and $\frac{\mathcal{T}}{\mathcal{T} + \mathcal{L}} = 0.66$ (with cavity mirror transmission \mathcal{T} and mirror loss \mathcal{L}) accounts for the outcoupling efficiency of an intracavity photon. M_s can be determined from the detected photon number and the independently measured detection-path efficiency (29). As shown in Fig. 4A, the distribution is double peaked, with the high-transmission peak with average source photon number $\langle M_s \rangle|_{n_g=0}$ corresponding no gate photon, whereas the gray area of low transmission $\langle M_s \rangle|_{n_g \geq 1}$ corresponds to the blocking by one or more gate photons. The optical gain per stored gate photon can then be defined as the gate-photon-induced change in source transmission, $G = \langle M_s \rangle|_{n_g=0} - \langle M_s \rangle|_{n_g \geq 1}$, which is directly determined from the measured histogram. The measured gain as a function of the applied source photon number is shown in Fig. 4B, in which the gain saturation occurring around 1000 source photons is likely due to optical pumping of the atom into magnetic sublevels with weaker cavity coupling. One stored gate photon can block more than ~ 600 source photons, of which ~ 400 are available outside the cavity.

In order to operate the device with gate retrieval in which the stored photon is recovered in the original optical mode after switching the source light, the source integration time was reduced to 1 μ s, which is less than the measured lifetime $\tau = (2.1 \pm 0.1) \mu$ s of the collective spin excitation. In this case, we can directly measure the cavity transmission probability conditioned on the detection of a gate photon, given by the gate-source cross-correlation function $g_{gs}^{(2)} =$

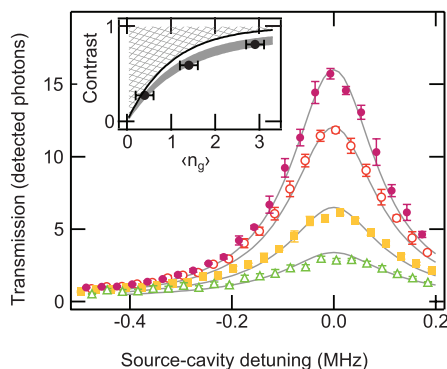


Fig. 2. Cavity transmission in the presence of stored gate photons. Average transmission spectra of a source beam applied for 24 μ s for mean stored gate photon numbers $\langle n_g \rangle = 0, 0.4, 1.4$, and 2.9 (top to bottom). The solid lines are theoretical curves (29). Error bars are SEM. (Inset) The relative transmission on cavity resonance (switching contrast) versus $\langle n_g \rangle$. The gray area indicates the theoretical prediction. The solid black line corresponds to the maximum average switching contrast that can be observed with coherent states of gate photons.

$\langle n_g n_s \rangle / (\langle n_g \rangle \langle n_s \rangle)$ in the limit $\langle n_g \rangle, \langle n_s \rangle \ll 1$. On cavity resonance, we measured $g_{gs}^{(2)} = 0.29^{+0.09}_{-0.08}$ for 0.2 average retrieved gate photons and 0.1 average source photons transmitted. These average photon values were chosen so as to minimize the two-photon probability in each beam while ensuring that the signal-to-background ratio remains sufficiently high. If we subtract independently measured detector backgrounds (29), we find a corrected value of $g_{gs}^{(2)} = 0.17^{+0.08}_{-0.06}$. This substantial anticorrelation, arising from the effective interaction between two initially uncorrelated photons of different wavelengths, is in good agreement with the value $T = 0.09 \pm 0.01$ deduced from Fig. 3B and the value $T = 0.16 \pm 0.06$ expected from first principles.

Last, we determined the available gain G_r in retrieval mode by measuring the retrieval reduction as a function of source photon number and display the result in Fig. 4E. In the process, it is only the scattering of a source photon into free space that reveals the location of the excited atom, collapsing the collective state into a single-atom state and preventing the retrieval. This scattering is suppressed in the strong-coupling

limit of cavity QED, and the observed dependence of retrieval on source photon number agrees well with the theoretical model. The physical gain of the device operated at $1/e$ retrieval reduction is $G_r = 2.2 \pm 0.2$, and the available gain outside the cavity is 1.4 ± 0.1 (lower owing to the 0.66 outcoupling efficiency). This demonstrates a gain exceeding unity in transistor operation in which the gate photon is preserved.

Our observations can be quantitatively understood in a simple cavity QED model: One atom in state $|s\rangle$ reduces the cavity transmission (1, 4) by a factor of $T = (1 + \eta)^{-2}$, where η is the single-atom cooperativity (30). In the strong-coupling regime of cavity QED, $\eta \gg 1$, already one stored gate photon can thus switch the source beam from transmission to reflection with high contrast. The cooperativity parameter η also governs the number of source photons that can be switched: The destruction probability for the collective excitation is given by the probability of scattering a photon into free space on the $|s\rangle \rightarrow |e\rangle$ transition. Such scattering probability is suppressed by cavity to $2\eta/(1 + \eta)^2$ in the regime of continuous cavity excitation (30). For $\eta \gg 1$, high transistor

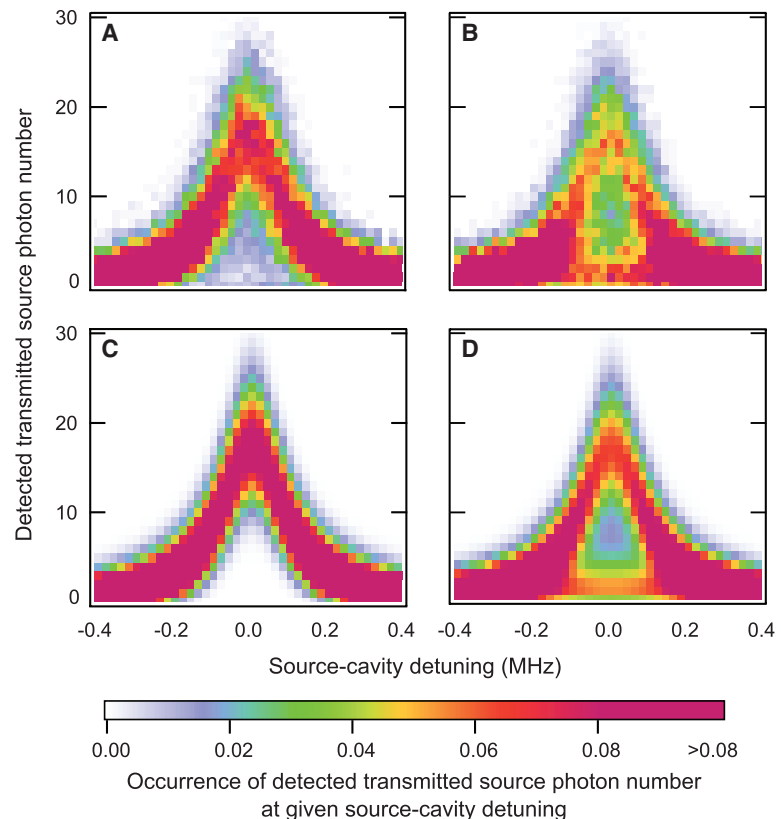


Fig. 3. Histogram of cavity transmission spectra. Cavity transmission (A) without and (B) with $\langle n_g \rangle = 0.5$ gate photons. The horizontal axis indicates the detuning of the source beam from the cavity resonance, and the vertical axis indicates the number of detected transmitted source photons in a 24- μ s detection window. The color indicates the occurrence rate of a particular detected transmitted source photon number for a given source-cavity detuning. The histogram displays a clear separation between the zero-gate-photon component $n_g = 0$ with high cavity transmission (17 detected source photons), and the component $n_g \geq 1$ ($n_g = 1$ with probability 0.8, $n_g > 1$ with 0.2) leading to cavity blocking (1.5 detected photons). (C and D) The corresponding theoretically expected histograms. The extinction factor $17/1.5$ for one gate photon is $T^{-1} = 11 \pm 1$.

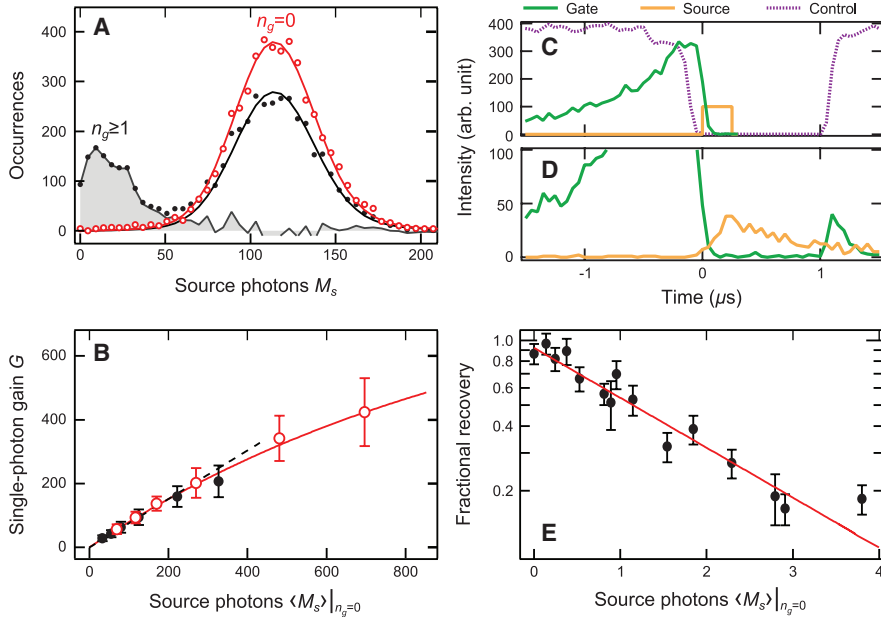


Fig. 4. Measurement of transistor gain. (A) Histogram of the integrated source photon number M_s in a 50- μ s window. The graph shows M_s for no applied gate photon ($n_g = 0$, open red circles) with a Poissonian fit and for a coherent state with $\langle n_g \rangle = 0.4$ stored gate photons (solid black circles). The gray area indicates the contribution from events with $n_g \geq 1$, with average value denoted by $\langle M_s \rangle|_{n_g \geq 1}$. (B) Transistor gain $G = \langle M_s \rangle|_{n_g = 0} - \langle M_s \rangle|_{n_g \geq 1}$ as a function of source strength $\langle M_s \rangle|_{n_g = 0}$ for integration times of 25 μ s (solid black circles) and 50 μ s (open red circles), with a linear fit to the first nine data points (black dashed line) and with exponential fit for gain saturation (red line). (C and D) Timing sequence for retrieval operation with (C) input pulses and (D) output pulses. (The actual gate, control, and source beam waveforms are shown, but relative powers are not to scale.) First, the control beam is adiabatically ramped down at $t = 0$ in order to store a gate photon in the atomic medium. Then, a source pulse is sent onto the cavity, and its transmission is measured. Subsequently, the control beam is adiabatically ramped up in order to retrieve and detect the gate photon. The combined storage and retrieval efficiency in the absence of source light after a storage time of 1 μ s is $(3.0 \pm 0.1)\%$. (E) Measurement of transistor gain in retrieval mode. The average fractional retrieval efficiency of the gate photon after 1 μ s is plotted versus $\langle M_s \rangle|_{n_g = 0}$ with an exponential fit. The fitted source photon number resulting in e^{-1} reduction is $M_{s0} = 1.9 \pm 0.1$ outside of the cavity ($M_{s0} = 2.8 \pm 0.2$ before out-coupling losses, which is in good agreement with the theoretical value 2.8 ± 0.1).

gain can be achieved, and the gate photon can be still retrieved from the atomic ensemble afterward. Because the cavity-blocking mechanism does not rely on the collective nature of the atomic excitation, even when the latter is destroyed, the remaining atom in state $|s\rangle$ continues to switch the source beam, leading to high gain $G \gg 1$ in the incoherent regime.

For the present system (5), the cooperativity for a two-level atom at an antinode is $\eta_0 = 8.6 \pm 0.4$. Averaging over polarization factors, the cavity standing wave, and the gate beam reduces the available cooperativity. The directly averaged cooperativity value is $\langle \eta \rangle = 2.8$, whereas the effective cooperativities for the transmission extinction and the attenuation photon number are $\eta_T = 1.5$ and $\eta_a = 3.3$, respectively (29). The theoretical model is in agreement with our measurements of the transmission reduction induced by one gate photon and with the measured dependence of gate-photon retrieval efficiency on source photon number, as displayed in Fig. 4E. The theoretical model, after including optical pumping into other magnetic sublevels (29), also

reproduces the measured cavity transmission histogram, as shown in Fig. 3D.

Our system constitutes a testbed in which we have explored the physical principles relevant to an all-optical transistor based on cavity QED with an atomic ensemble. Before it can be used as a practical device, it will be necessary to improve the input and output coupling efficiencies for the gate and source photons, which limit the usable gain in the system. The combined storage and retrieval efficiency of 3% for the gate photon is limited primarily by the optical density. The latter could be improved by using a deeper trap, in combination with further cooling of the atomic ensemble, which would also increase the gate-photon storage time that is currently limited by Doppler broadening. The cavity outcoupling efficiency for the source photons of 0.66 could be improved to 0.97 by using state-of-the-art mirrors (1, 2, 4).

The present work opens up new perspectives for all-optical information processing with strong deterministic interactions between initially uncorrelated, distinguishable photons. The gain

$G_T > 1$ in operation with gate photon retrieval may enable not only hitherto unexplored all-optical quantum circuits with feedback and gain, but also the nondestructive detection of the gate photon—a feat that has so far only been accomplished for microwave photons confined in a cavity (31). The correlations between one gate and multiple source photons produced by the effective photon-photon interaction can be used to create two-mode entangled states of many photons. Last, cavities with larger cooperativity (1–4) may enable high-fidelity deterministic photonic quantum gates.

References and Notes

1. K. M. Birnbaum *et al.*, *Nature* **436**, 87–90 (2005).
2. F. Brennecke *et al.*, *Nature* **450**, 268–271 (2007).
3. Y. Colombe *et al.*, *Nature* **450**, 272–276 (2007).
4. A. Kubanek *et al.*, *Phys. Rev. Lett.* **101**, 203602 (2008).
5. H. Tanji-Suzuki, W. Chen, R. Landig, J. Simon, V. Vuletić, *Science* **333**, 1266 (2011).
6. D. W. Brooks *et al.*, *Nature* **488**, 476–480 (2012).
7. P. Michler *et al.*, *Science* **290**, 2282–2285 (2000).
8. D. Press *et al.*, *Phys. Rev. Lett.* **98**, 117402 (2007).
9. I. Fushman *et al.*, *Science* **320**, 769–772 (2008).
10. T. Volz *et al.*, *Nat. Photonics* **6**, 605–609 (2012).
11. R. Bose, D. Sridharan, H. Kim, G. S. Solomon, E. Waks, *Phys. Rev. Lett.* **108**, 227402 (2012).
12. Y. O. Dudin, A. Kuzmich, *Science* **336**, 887–889 (2012).
13. T. Peyronel *et al.*, *Nature* **488**, 57–60 (2012).
14. J. Hwang *et al.*, *Nature* **460**, 76–80 (2009).
15. M. Bajcsy *et al.*, *Phys. Rev. Lett.* **102**, 203902 (2009).
16. H.-Y. Lo *et al.*, *Phys. Rev. A* **83**, 041804(R) (2011).
17. H. Schmidt, A. Imamoglu, *Opt. Lett.* **21**, 1936–1938 (1996).
18. A. Imamoglu, H. Schmidt, G. Woods, M. Deutsch, *Phys. Rev. Lett.* **79**, 1467–1470 (1997).
19. S. Harris, Y. Yamamoto, *Phys. Rev. Lett.* **81**, 3611–3614 (1998).
20. M. Fleischhauer, M. D. Lukin, *Phys. Rev. Lett.* **84**, 5094–5097 (2000).
21. M. Fleischhauer, A. Imamoglu, J. P. Marangos, *Rev. Mod. Phys.* **77**, 633–673 (2005).
22. B. Dayan *et al.*, *Science* **319**, 1062–1065 (2008).
23. Q. A. Turchette, C. J. Hood, W. Lange, H. Mabuchi, H. J. Kimble, *Phys. Rev. Lett.* **75**, 4710–4713 (1995).
24. R. J. Thompson, G. Rempe, H. J. Kimble, *Phys. Rev. Lett.* **68**, 1132–1135 (1992).
25. D. E. Chang, A. S. Sørensen, E. A. Demler, M. D. Lukin, *Nat. Phys.* **3**, 807–812 (2007).
26. C. Liu, Z. Dutton, C. H. Behroozi, L. V. Hau, *Nature* **409**, 490–493 (2001).
27. D. F. Phillips, A. Fleischhauer, A. Mair, R. L. Walsworth, M. D. Lukin, *Phys. Rev. Lett.* **86**, 783–786 (2001).
28. A. V. Gorshkov, A. André, M. Fleischhauer, A. S. Sørensen, M. D. Lukin, *Phys. Rev. Lett.* **98**, 123601 (2007).
29. Materials and methods are available as supplementary materials on Science Online.
30. H. Tanji-Suzuki *et al.*, *Adv. At. Mol. Opt.* **60**, 201–237 (2011).
31. C. Guerlin *et al.*, *Nature* **448**, 889–893 (2007).

Acknowledgments: This work was supported by NSF and the Air Force Office of Scientific Research. K.M.B. gratefully acknowledges support from NSF through the Graduate Research Fellowship (0645960). R.B. gratefully acknowledges support from the Fonds zur Förderung der wissenschaftlichen Forschung through the doctoral program CoQuS (W1210).

Supplementary Materials

www.sciencemag.org/cgi/content/full/science.1238169/DC1
Materials and Methods
Supplementary Text
Fig. S1
Table S1
References and Notes

22 March 2013; accepted 24 June 2013
Published online 4 July 2013;
10.1126/science.1238169

This copy is for your personal, non-commercial use only.

If you wish to distribute this article to others, you can order high-quality copies for your colleagues, clients, or customers by [clicking here](#).

Permission to republish or repurpose articles or portions of articles can be obtained by following the guidelines [here](#).

The following resources related to this article are available online at www.sciencemag.org (this information is current as of September 7, 2015):

Updated information and services, including high-resolution figures, can be found in the online version of this article at:

<http://www.sciencemag.org/content/341/6147/768.full.html>

Supporting Online Material can be found at:

<http://www.sciencemag.org/content/suppl/2013/07/03/science.1238169.DC1.html>

A list of selected additional articles on the Science Web sites **related to this article** can be found at:

<http://www.sciencemag.org/content/341/6147/768.full.html#related>

This article **cites 30 articles**, 5 of which can be accessed free:

<http://www.sciencemag.org/content/341/6147/768.full.html#ref-list-1>

This article has been **cited by** 6 articles hosted by HighWire Press; see:

<http://www.sciencemag.org/content/341/6147/768.full.html#related-urls>

This article appears in the following **subject collections**:

Physics, Applied

http://www.sciencemag.org/cgi/collection/app_physics